Formation of Nanostructured PVDF/PA11 Blends Using High-Shear Processing

Hiroshi Shimizu,*,† Yongjin Li,† Akira Kaito,† and Hironari Sano‡

National Institute of Advanced Industrial Science and Technology, Nanotechnology Research Institute, Tsukuba Central 5, 1-1-1 Higashi, Tsukuba, Ibaraki 305-8565, Japan, and Mitsubishi Chemical, Science and Technology Research Center, 1000 Kamoshida-cho, Aoba-ku, Yokohama 227-0033, Japan

Received June 29, 2005
Revised Manuscript Received August 5, 2005

A growing fraction of plastic resins produced today are blends of two or more polymers.[1] Polymer blending offers an extraordinary rich range of new materials with enhanced characteristics regarding mechanical, chemical, or optical performances. However, most commercial blends are immiscible because nearly all polymer pairs cannot be soluble in each other. When two immiscible polymers are blended during melt extrusion, a stable morphology is reached in which one phase is mechanically dispersed inside the other. The size and shape of the dispersed phase depend on several processing parameters, including rheological and interfacial properties and the composition of the blend. By using the conventional mixing machines, the experimental limitation of domain size has been reported to be approximately 100 and 350 nm for Newtonian systems[2−6] and polymer blend systems,[7,8] respectively. Several methods[9−17] of reducing phase size and improving interfacial adhesion for the practical application of polymer blend materials have been developed. Currently, a phase structure on the micrometer or submicrometer scale, that is, microstructured blends, is technically easy to prepare using typical processing methods, such as extrusion or injection molding. However, the preparation of nanostructured polymer blends for immiscible polymers, with a phase size of less than 100 nm, is very challenging using normal processing methods currently available. Very recently, nanostructured blends have been produced from block copolymers by using conventional melt processing,[18,19] but the method shows obvious limitation for the practical application.

One of the authors has very recently studied the in-situ phase behavior of polymer blends under a high-shear flow field.[20] It was found that immiscible poly(*p*-phenylene sulfide)/polyamide 46 blends show a miscible region under a flow field with a high shear rate above 1000 s^{-1}. Moreover, the miscible region was enlarged by a higher shear rate of 3000 s^{-1}. Therefore, processing under high-shear flow is considered to be a very effective technique for making the immiscible polymer blends miscible. On the basis of the obtained results, the high-shear extruder HSE3000mini has been developed. The extruder can reach a maximum screw rotation speed of 3000 rpm. Furthermore, the specially designed feedback-type screw (L/D = 1.78) has been used to make the sample to circulate in the extruder during melt mixing. The sample feed at the top of the screw was back soon at the root of the screw through the feedback path. By using this new high-shear extruder with the capability about 5 mL, PVDF and PA11 were directly melt-blended. It is found that PA11 can be dispersed in the PVDF phase with a domain size of several tens of nanometers, which is the first example of a nanostructured polymer blend obtained by a simple mechanical method.

Experimental Section. Poly(vinylidene fluoride) (PVDF) and polyamide 11 (PA11) used were commercially available KF850 (Kureha Chemical, Japan) and Rilsan BMN-O (Atfina Co., Ltd.), respectively. All the polymers were dried in a vacuum oven at 100 °C for 12 h before processing.

High-shear processing was performed using a high-shear extruder, HSE3000mini (Imoto, Co. Japan). A feedback-type screw was used in this extruder. The L/D ratio of the screw was about 1.78. The rotation speed of the screw used in this study was 1200 rpm, which corresponds to the average shear rate of 1760 s^{-1} at the region of top part of the screw. The mixing time was varied from 1 to 4 min in this work. No apparent degradation occurs under the present processing conditions from the appearance (sample color) of the obtained blends. Mixed pellets of the two polymers (PVDF/PA11) were melt-blended at 230 °C for the desired mixing time using the extruder, and then the sheets (0.2 mm thickness) were extruded from a T-die. The viscosity ratio between PVDF and PA11 has been measured to be about 1.61 at 230 °C when the shear rate is about 1500 s^{-1}. To compare the dispersed structure of the blend, a normal (low shear) extruder was also used in this study. The rotation speed of the screw in a normal extruder at 100 rpm was estimated to be a shear rate of 50 s^{-1}.

The sections of the PVDF/PA11 blends were observed and analyzed in a high accelerating voltage transmission electron microscopy (TEM), TECNAI G2-F20 (FEI Co.) equipped with an energy-dispersive X-ray (EDX) microanalysis system at 200 kV. For TEM-EDX analysis, electron beams were irradiated to a small spot (diameter 10 nm) and the emitted X-rays were analyzed with the specific EDX spectra counts for 10 s. For TEM observation, the sample was stained in the vapor phase. First, the trimmed specimen embedded in epoxy resin was stained with solid OsO_4 for 2 h in a sealed glass tube. Next, the corresponding specimen was stained with solid RuO_4 for 15 min. Then, the stained specimen for TEM was cut into about 120 nm sections with an ultramicrotome Reichert ULTRACUT-UCT and a Diatome diamond knife.

Small-angle X-ray scattering (SAXS) patterns were obtained using microfocused Cu Kα radiation (45 kV, 60 mA) generated by an X-ray diffractometer (Rigaku Ultax 4153 A 172B) and an imaging plate detector. The extruded samples were directly used for SAXS measurements. The exposure time is 4 h for each measurement.

The stress−strain curves were measured using a tensile testing machine, Tensilon UMT-300 (Orientec

† Nanotechnology Research Institute.
‡ Mitsubishi Chemical, Science and Technology Research Center.
* To whom correspondence should be addressed: e-mail Shimizu-hiro@aist.go.jp; Tel (+81)-29-861-6294; Fax (+81)-29-861-6294.

10.1021/ma051395f CCC: $30.25
Published on Web 08/18/2005

Co. Ltd). Dumbbell-shaped specimens were punched from the extruded sample for the tensile test. Tensile tests were carried out at a rate of 5 mm/min at 20 °C and 50% relative humidity.

Dynamic mechanical properties of all samples were measured with RHEOVIBRON DDV-25FP-S (Orientec Co. Ltd.) in a stretching mode. The dynamic storage and loss moduli were determined at a frequency of 10 Hz and a heating rate of 3 °C/min as a function of temperature from −150 to 175 °C.

Results and Discussion. Figure 1a shows a typical TEM image for the high-shear-processed PVDF/PA11 blend. The sample was processed by the high-shear extruder at 230 °C for 4 min (screw rotation speed of 1200 rpm). In this figure, PA 11 is observed as a dark phase and PVDF is observed as a white phase because PA11 is more readily stained than PVDF. As shown in Figure 1a, the nanosized PA11 domains (the dark phase) are estimated to be 20−100 nm, and they are dispersed precisely in the PVDF phase. Moreover, the PA11 lamellar structure was observed clearly in the TEM image. This type of nanodispersed structure of blends is the first example in the world obtained using a simple mechanical blending method without adding compatibilizers to our knowledge. The domain size of the blend is much smaller than 350 nm, which corresponds to the experimental limit until now by using the conventional processing techniques. In addition, the experiments show that the PA11 nanodomain size is hardly affected by mixing time and blend component ratio, while the number of nanodomains is significantly increased by prolonging mixing time. It is worth noting that nanostructured PVDF/PA11 blends are very stable thermodynamically against thermal annealing. The blend structure processed at a high shear was unchanged by the remelt conditions.

To elucidate the component interactions for the high-shear-processed blend, energy-dispersive X-ray (EDX) microanalysis was used for elemental analysis of each part in Figure 1a. Figure 1b,c shows the EDX spectra of the respective parts designated in Figure 1a. In these figures, the horizontal axis represents the energy corresponding to the specific X-ray emitted and the vertical axis represents intensity counts of the X-ray. In Figure 1b,c, the most intense peak observed at 0.28 keV was assigned to the specific X-ray of carbon (C). The relatively intense peaks originating from nitrogen (N) at 0.39 keV and oxygen (O) at 0.52 keV were clearly observed in the PVDF phase designated in Figure 1a, which suggest that the PA11 chains are mixed with the PVDF chains in the nanospots with a diameter of 10 nm. Although the stained PA11 domain was only observed in the other spot of Figure 1a, an intense peak originating from fluorine (F) was clearly observed at 0.67 keV in the EDX spectrum of Figure 1c. This result indicates that the PVDF chains interpenetrated in the PA11 domain. The TEM-EDX results suggest that both the PVDF and PA11 chains mixed with each other after the high-shear processing. Therefore, the miscibility between PVDF and PA11 was improved by the high-shear processing to form a partially miscible state with the nanosize dispersion.

TEM-EDX investigation has shown the molecular chain interpenetrating state for the high-shear-processed blend because of the coexistence of F, N, and O within the nanospots with a diameter of about 10 nm. Small-angle X-ray scattering (SAXS) was used to elucidate the lamellar structures of the prepared novel nanoblend. Figure 2 shows the Lorentz-corrected SAXS

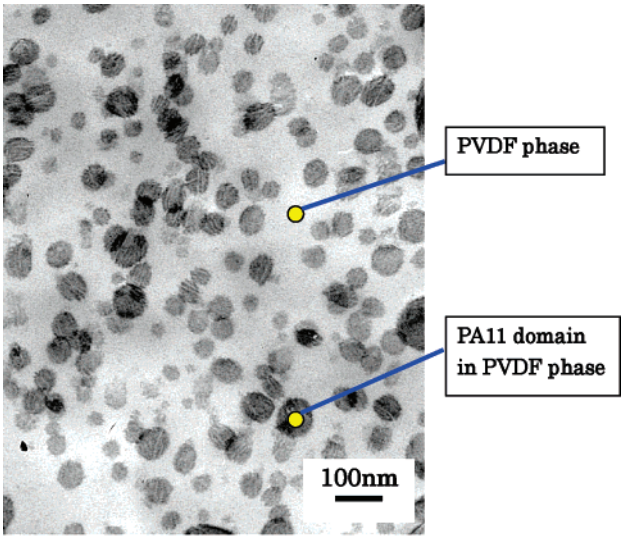

(a)

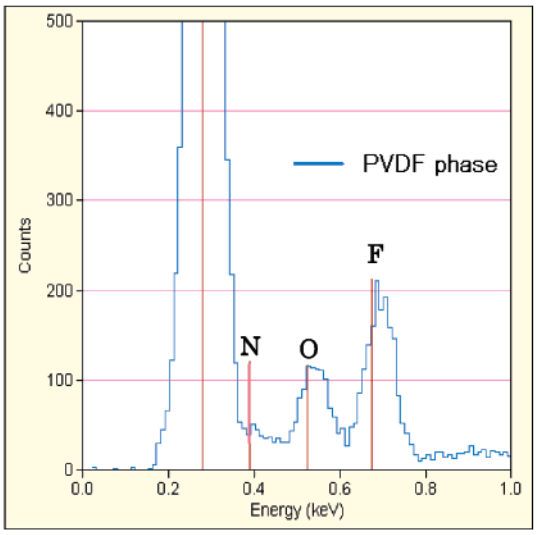

(b)

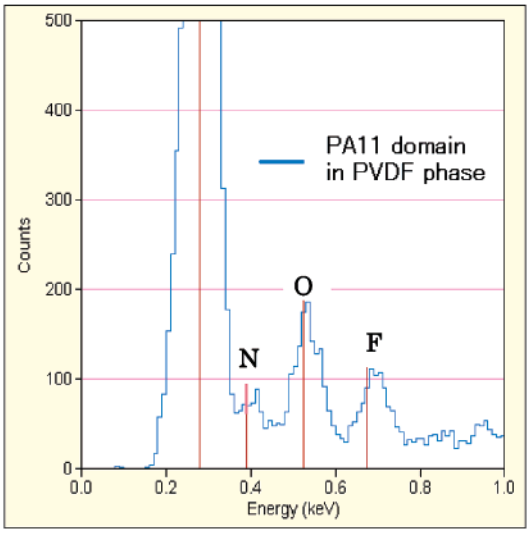

(c)

Figure 1. TEM image (a) and TEM-EDX spectra (b, c) of PVDF/PA11 = 80/20 blend processed at 230 °C for 4 min (screw rotation speed of 1200 rpm).

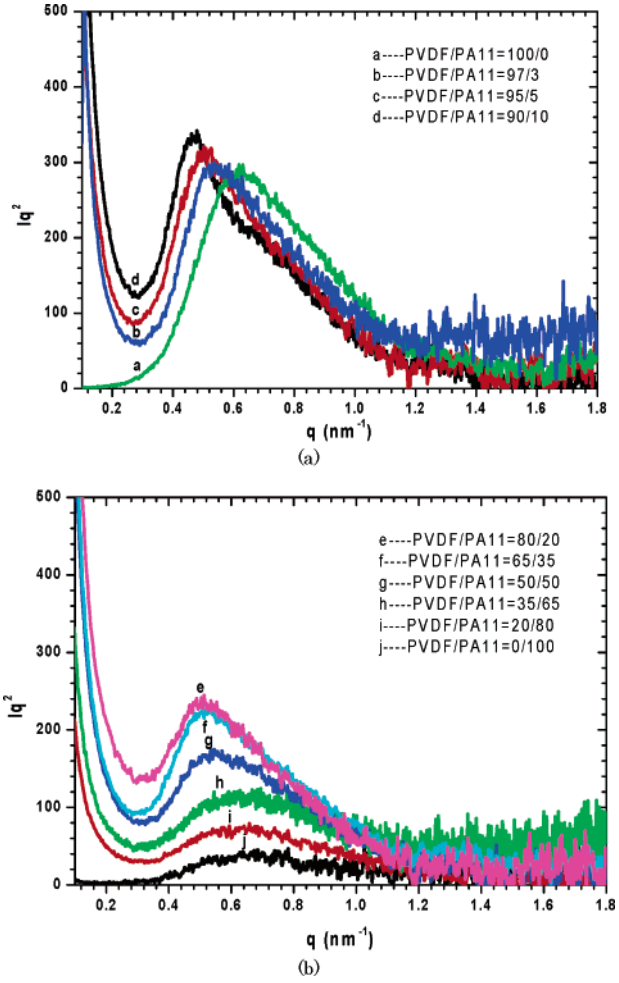

Figure 2. SAXS profiles of PVDF, PA11, and PVDF/PA11 nanoblends at room temperature.

profiles of PVDF/PA11 nanoblends with various component ratios. SAXS intensity was normalized by thickness and exposure time after subtracting air scattering. PVDF exhibits a higher scattering peak than PA11 because of its higher electron density contrast between its alternating crystalline and amorphous layers. By comparing the scattering curves of the blends and pure polymers, it can be seen from Figure 2 that all the high-shear-processed blends show a very strong scattering in the low-scattering-angle region ($q < 0.1$ nm^{-1}), termed "zero-angle scattering". The strong "zero-angle scattering" indicates the nanodomains in the blends. The scattering intensity of this "zero-angle scattering" monotonically decreases as a function of the scattering vector characteristic of a spherical morphology, where the spheres (domains) are randomly arranged in space, which is consistent with the TEM results in Figure 1a.

The average long period (L), crystalline lamella thickness (L_c), and amorphous layer thickness (L_a) can be calculated by a one-dimensional correlation function

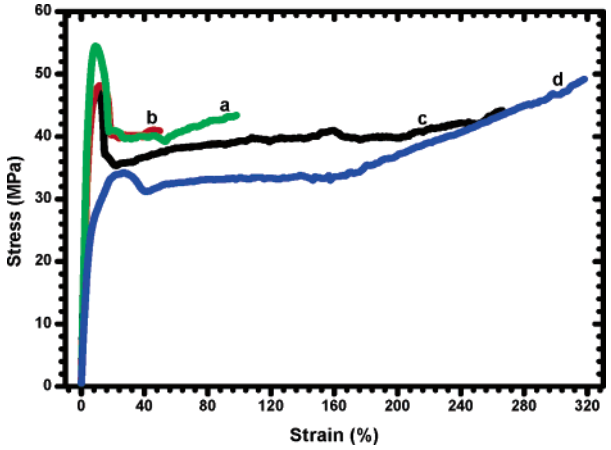

Figure 3. Stress−strain curves of neat PVDF (a), PVDF/PA11 = 80/20 blends processed at low shear (b), PVDF/PA11 = 80/20 blends processed at high shear (c), and neat PA11 (d).

method from Figure 2, assuming a dual phase model for crystalline polymers.[21] Table 1 gives the changes in the three average parameters as functions of the composition ratio of the nanoblend as well as that of the same blend processed at a low shear rate. The fact that the high-shear-processed blend samples show an enlarged long period and an amorphous layer thickness indicates the chain incorporation between PVDF and PA11 during the high-shear processing. These results are highly consistent with those of the TEM-EDX analysis. In contrast, there is no change in the long period for the low-shear-processed sample, indicating the immiscibility between PVDF and PA11 at a low shear rate. From the results of SAXS and TEM-EDX measurements, it is suggested that PVDF and PA11 molecular chains insert into the amorphous region of the other component and result in an extended long period of the lamellar structure.

Figure 3 shows the stress−strain curves of neat PVDF (a), PVDF/PA11 = 80/20 blends processed at a low shear (b), PVDF/PA11 = 80/20 blends processed at a high shear (c), and neat PA11 (d). The yield stress of the PVDF/PA11 = 80/20 blend processed at a high shear was almost the same as that of the blend processed at a low shear. Compared with the blend processed at a low shear, however, the nanostructured blend processed at a high shear shows significantly increased elongation at breakup. It is found that the elongation at breakup of the nanostructured PVDF/PA11 blend is about 560% higher than that of the same blend prepared under low shear. It is worth noting that the ductility of the nanostructured blend with a small amount of PA11 (20 wt %) is almost equal to that of neat PA11.

The storage modulus and the glass transition temperature of the obtained nanostructure blend have been investigated and compared with those of the low-shear-processed sample by the DMA experiments, as shown in Figure 4. The storage modulus of the high-shear-

Table 1. Average Structure Parameters for PA11/PVDF Blends Prepared by High-Shear (with a Shear Rate about 1760 s^{-1}) and Low-Shear (with a Shear Rate about 50 s^{-1}) Processing Calculated by One-Dimensional Correlation Function[a]

PA11/PVDF	100/0	80/20	65/35	50/50	35/65	20/80	10/90	5/95	3/97	0/100	50/50[b]
L (nm)	11.0	11.9	12.2	12.5	13.0	13.5	13.9	12.4	11.7	10.6	10.4
L_c (nm)	4.1	4.3	4.3	4.4	4.7	5.1	5.2	4.1	3.8	3.6	3.9
L_a (nm)	6.9	7.6	7.9	8.1	8.3	8.4	8.7	8.3	7.9	7.0	6.5

[a] L = average long period, L_c = average crystalline thickness, and L_a = average amorphous part thickness. [b] Low-shear-processed sample for comparison.

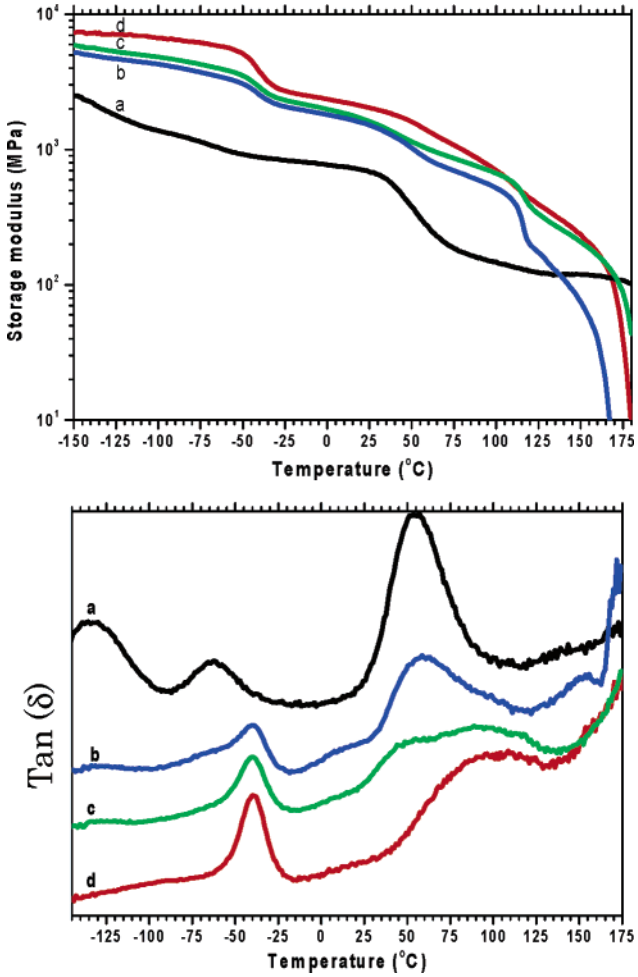

Figure 4. Temperature dependence of the dynamic storage modulus and tan(δ) for neat PA11 (a), PVDF/PA11 = 80/20 blends processed at low shear (b), PVDF/PA11 = 80/20 blends processed at high shear (c), and neat PVDF (d).

processed blend is higher than that of the low-shear-processed same blend in the whole temperature range. The high-shear-processed blend showed an excellent behavior in the storage modulus curve at the higher temperature region than that of the low-shear-processed blend. On the other hand, the glass transition temperature (T_g) of the blend was found to be dependent greatly upon the processing shear rate. As shown in Figure 4, the T_g of neat PA11 is observed at about 52 °C. The T_g of the low-shear-processed blend is observed at the same temperature of neat PA11, while that of the high-shear-processed sample is remarkably shifted to about 43 °C, indicating the improved miscibility between the two components by the high-shear processing.

To summarize, we have found that high-shear processing without additives can lead to the production of stable nanostructured blends with properties impossible for classical blends to achieve. Here, we demonstrated for the first time the successful preparation of a nanostructured polymer blend, a poly(vinylidene fluoride) (PVDF)/polyamide 11 (PA11) system, in which the PA11 domains with a size of several tens of nanometers are dispersed in the PVDF phase and the nanostructured blends can be produced with a wide range of compositions. The nanostructured polymer blend has a unique combination of properties such as excellent ductility and mechanical properties, which are impossible to achieve with classical processing. Such a novel and simple strategy should be widely applicable to the processing of other immiscible polymer blends. Soon, the approach developed here will provide various methods of preparing other new materials, which will lead to new applications of already existing polymers.

Acknowledgment. This work was supported by the New Energy and Industrial Technology Development Organization (NEDO) for the "Project on Nanostructured Polymeric Materials".

References and Notes

(1) Utracki, L. A. *Polymer Blends Handbook*; Kluwer Academic Dortrecht: Boston, 2003.
(2) Taylor, G. I. *Proc. R. Soc. London* **1932,** *A138,* 41−48.
(3) Taylor, G. I. *Proc. R. Soc. London* **1934,** *A146,* 501−523.
(4) Grace, H. P. *Chem. Eng. Commun.* **1982,** *14,* 225−277.
(5) Rumscheidt, F. D.; Mason, S. G. *J. Colloid Sci.* **1961**, *16,* 238−261.
(6) Serpe, G.; Jarrin, J.; Dawans, F. *Polym. Eng. Sci.* **1990**, *30,* 553−564.
(7) Wu, S. *Polym. Eng. Sci.* **1987,** *27,* 335−343.
(8) Uttandaraman, S.; Macosko, C. W. *Macromolecules* **1995,** *28,* 2647−2657.
(9) Park, I.; Barlow, J. W.; Paul, D. R. *J. Polym. Sci., Part B: Polym. Phys.* **1992,** *30,* 1021−1033.
(10) Wildes, G. S.; Harada, T.; Keskkula, H. *Polymer* **1999**, *40,* 3069−3082.
(11) Frisch, H. L.; Frisch, K. L.; Klempner, D. *Polym. Eng. Sci.* **1974**, *14,* 646−650.
(12) Robeson, L. M.; Furtek, A. B. *J. Appl. Polym. Sci.* **1979**, *23,* 645−659.
(13) Paul, D. R. *Macromol. Symp.* **1994,** *78,* 83−93.
(14) Charoensirisomboon, P.; Inoue, T.; Weber, M. *Polymer* **2000**, *41,* 4483−4490.
(15) Ibuki, J.; Charoensirisomboon, P.; Chiba, T.; Ougizawa, T.; Inoue, T.; Weber, M.; Koch, E. *Polymer* **1999**, *40,* 647−653.
(16) Pernot, H.; Baumert, M.; Court, F.; Leibler, L. *Nat. Mater.* **2002**, *1,* 54−58.
(17) Hu, G. H.; Cartuer, H.; Plummer, C. *Macromolecules* **1999**, *32,* 4713−4718.
(18) Koulic, C.; Jerome, R. *Macromolecules* **2004**, *37*, 888−893.
(19) Koulic, C.; Jerome, R. *Macromolecules* **2004**, *37*, 3459−3469.
(20) Shimizu, H.; Komori, K.; Inoue, T. *Trans. Mater. Res. Soc. Jpn.* **2004**, *29,* 263−265.
(21) Strobl, G. R.; Schneider, M. J. *J. Polym. Sci., Polym. Phys.* **1980,** *18,* 1343−135.

MA051395F